Sensing and Bio-Sensing Research 4 (2015) 40–45

Contents lists available at ScienceDirect

Sensing and Bio-Sensing Research

journal homepage: www.elsevier.com/locate/sbsr

A new device for liver cancer biomarker detection with high accuracy

Shuaipeng Wang [a,b], Jingjing Wang [a,b], Yinfang Zhu [a,b], Jinling Yang [a,b,*], Fuhua Yang [a]

[a] Institute of Semiconductors, Chinese Academy of Sciences, Beijing 100083, PR China
[b] State Key Laboratory of Transducer Technology, Shanghai 200050, PR China

ARTICLE INFO

Keywords:
MEMS cantilever
Liver cancer biomarker
Mass detection
Local reaction
Adsorption-induced stiffness change

ABSTRACT

A novel cantilever array-based bio-sensor was batch-fabricated with IC compatible MEMS technology for precise liver cancer bio-marker detection. A micro-cavity was designed in the free end of the cantilever for local antibody-immobilization, thus adsorption of the cancer biomarker is localized in the micro-cavity, and the adsorption-induced k variation can be dramatically reduced with comparison to that caused by adsorption of the whole lever. The cantilever is pizeoelectrically driven into vibration which is pizeoresistively sensed by Wheatstone bridge. These structural features offer several advantages: high sensitivity, high throughput, high mass detection accuracy, and small volume. In addition, an analytical model has been established to eliminate the effect of adsorption-induced lever stiffness change and has been applied to precise mass detection of cancer biomarker AFP, the detected AFP antigen mass (7.6 pg/ml) is quite close to the calculated one (5.5 pg/ml), two orders of magnitude better than the value by the fully antibody-immobilized cantilever sensor. These approaches will promote real application of the cantilever sensors in early diagnosis of cancer.

1. Introduction

Recently, MEMS-based technologies are playing more and more important roles in early diagnosis of cancer due to their high sensitivity, fast response, low cost, small reagent consumption, portability, real-time, label-free detection, and so on. Several methods for detecting serum biomarkers have been developed, for example, surface plasmon resonance (SPR), quartz crystal microbalance (QCM), and micro-cantilevers, etc [1]. Among them, cantilever sensors are the most attractive candidate for practical application in early diagnosis of cancer from the viewpoint of batch-fabrication, cost, and reliability [2–5].

For the cantilever sensor working in a dynamic mode, the resonance frequency shift depends on variation of mass m and lever stiffness k. However, in conventional cantilever sensors working on mass-loading principle, the effect of k change is neglected, this results in distinct error for mass detection [6]. Lee J. H. found that the measured frequency change (184 Hz) is two orders of magnitude larger than the theoretical value according to mass loading of C-reactive protein (2 Hz) [7]. Similar results was reported by Gupta A. K., the calculated frequency change (24 kHz) is 5 times smaller than the experimental value (132 kHz), and it was experimentally demonstrated that the frequency change depended crucially on the attachment kinetics of biomolecules on the cantilever [8].

Adsorption-induced surface stress made substantial contribution to the detection error. Both theoretical and experimental studies have been undertaken to investigate the effect of surface stress in microcantilevers. Hwang et al. reported that molecular interactions generate surface stress on the microcantilever surface and modify the lever stiffness, but it is difficult to distinguish the frequency shift caused by mass loading and the stiffness variation from the measured frequency change of 100–600 Hz responding to the antigen concentrations of 10 and 100 ng/ml [9]. Wang et al. studied the effect of gas adsorption-induced surface stress on mechanical properties of ultra-thin silicon cantilever with different orientations, but no quantitative description on the adsorption-induced stress is included [10]. Nevertheless, until now, there is no feasible method to quantitatively estimate the effect of surface stress on the accuracy for mass detection, although it is essential for practical application of cantilever-based biosensors in mass detection with high sensitivity.

In this paper, a novel cantilever arrays sensor is batch-fabricated for precise bio-marker detection. A local biochemical reaction cavity is designed in the free end of the cantilever to reduce the effect of k variation with adsorption. And an analytical model integrating the adsorption-induced surface stress has been established to eliminate the effect of k change on mass detection

* Corresponding author at: Institute of Semiconductors, Chinese Academy of Sciences, Beijing 100083, PR China. Tel.: +86 10 8230 4700.
E-mail address: jlyang@semi.ac.cn (J. Yang).

http://dx.doi.org/10.1016/j.sbsr.2014.10.002
2214-1804/

accuracy. These modifications have dramatically improved the performance of the fabricated biosensor, which is capable of sensing the liver cancer biomarker-AFP with high accuracy.

2. Material and method

2.1. Fabrication

Fig. 1 shows the illustration of the device. Cantilever arrays are designed to jointly detect multi-biomarkers. The cantilever is driven by piezo and the response signal is piezoresistively sensed and detected by Wheatstone bridge circuits. The reference cantilever is designed to eliminate the influence of non-specific adsorption and environment noise. In order to reduce the effect of the adsorption-induced k change, the micro-cavity are designed in the free end of the cantilever to serve for local interaction with the antigen. The pillar arrays in the micro-cavity are made for increasing detection upper limit. These structural features offer several advantages: high mass detection accuracy, high throughput, small volume for portable system.

The device is batch fabricated with CMOS compatible processes. The ⟨100⟩ oriented n-type silicon top layer of 4-inch SOI wafer has a thickness of 5 μm. Fig. 2 gives the schematic of fabrication processes. Firstly, a 200 nm thick SiO_2 layer is grown by dry oxidation to serve as the mask for ion implantation, and an additional SiO_2 mask layer is deposited by plasma enhanced chemical-vapor deposition (PECVD) on the backside for deep etching in step (a). Then boron implantation is done for making the piezoresistors and the electrical lines, and is followed by annealing at 1000 °C. Next, the top Si layer is etched by reactive ion etching (RIE) to define the local reaction cavity in step (b). In step (c), the cantilevers are shaped by RIE. Lift-off is done to make the Cr/Au electrodes in step (d) and a PECVD SiO_2 mask is made on the front side of the wafer to protect the cantilevers in step (e). Subsequently the Si substrate is etched to define the chip body from the backside by deep reactive ion etching (DRIE) until a desired depth, and an isotropy RIE is employed to remove the residual Si substrate from the front side of the wafer. Finally, the cantilevers are released by BOE in step (f). The SEM pictures of the device are shown in Fig. 3.

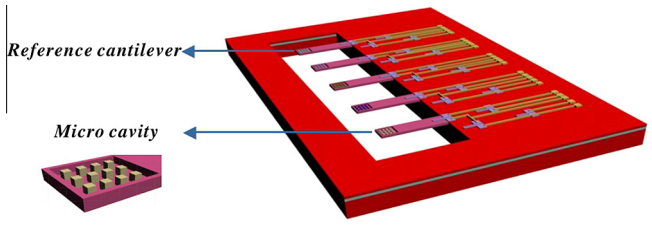

Fig. 1. Illustration of the cantilever arrays, the micro-cavity on the free end of the cantilever with pillar arrays.

2.2. Functionalization of the cantilever

The functionalization process of the cantilever and the locally immobilized lever with AFP antibody are depicted in Fig. 4(a) and (b). The silicon cantilever is oxidized using oxygen plasma and subsequently silanized at 24 °C using a 10% 3-aminopropyltriethoxysilane (APTES) solution in ethanol for 1 h. Freshly silanized-cantilever is incubated at 24 °C in 5% glutaraldehyde GA solution for 1 h to form a stable bond between $–NH_2$ and –CHO and then washed in phosphate buffered saline (PBS, pH 7.4), thus the cantilever is able to bind with protein (three times washing in buffer is done for all the cantilevers). Then the fluorescent Cy-5 labeled immunoglobulin G (IgG) antibody at a concentration of 40 μg/mL is locally immobilized in the micro-cavity of the lever by micro printing technology and incubated for 1 h and whereafter the levers are washed in PBS, as shown in Fig. 4(b). The micro printing system can print various antibodies on different cantilever at wafer level to ensure simultaneous detection of multiple biomarkers. The other active site of the cantilever is terminated by bovine serum albumin (BSA) solution at 24 °C over night, thus only antibody-bounded micro-cavity could capture the AFP antigen. For comparison, the IgG antibody was immobilized on the whole surface of some cantilevers. IgG is purchased from the company of Thermo (Massachusetts, USA).

The mechanical properties of the cantilevers were characterized by laser Doppler vibration system. Fig. 5 is a typical resonance spectrum of the cantilever. The quality factors (Q) of the cantilever are 587 in air and 49,434 in vacuum, good enough for achieving high sensitivity. For the cantilever of l = 195 μm, w = 75 μm, and h = 5 μm, the sensitivity and the mass resolution are 0.31 pg/Hz and 0.075 pg, respectively, high enough for early diagnosis of cancer.

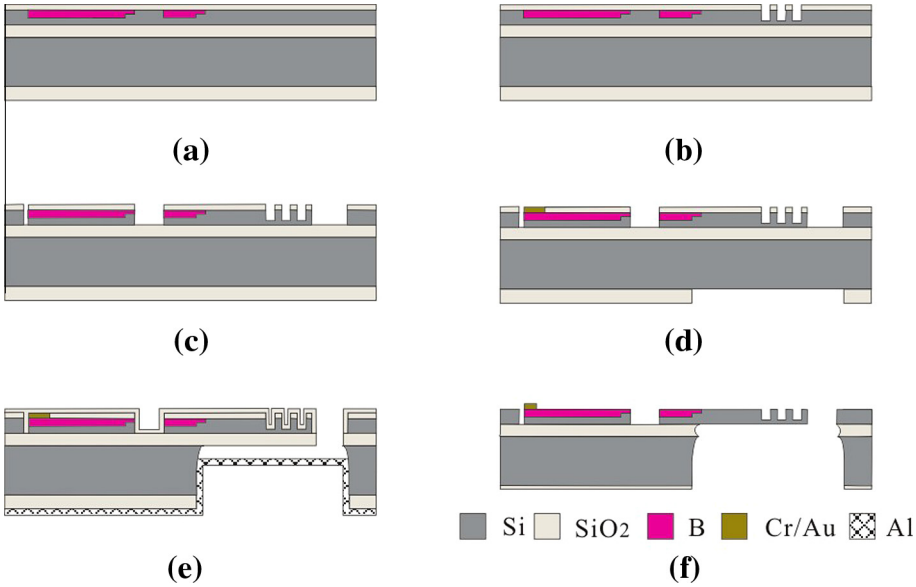

Fig. 2. Fabrication process flow of the cantilever.

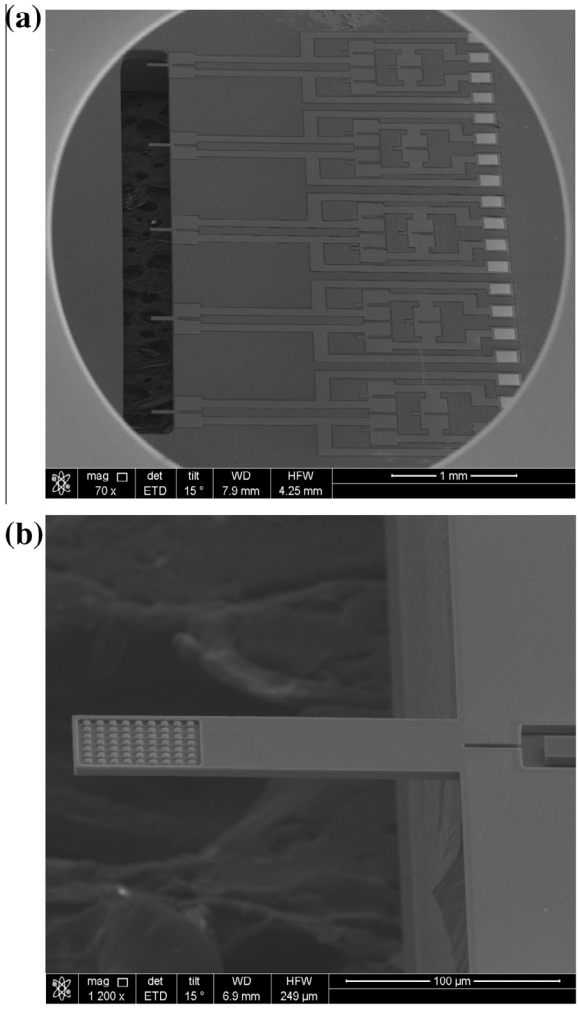

Fig. 3. (a) Cantilever array, (b) Enlarged view of the cantilever.

3. Results and discussion

3.1. Mass resolution of cantilever

The resonance frequency of the cantilever working at dynamic mode is given by:

$$f = \frac{1}{2\pi}\sqrt{\frac{k}{m^*}}, \tag{1}$$

Assuming that the lever stiffness k does not depend on adsorption, the sensitivity $\Delta m/\Delta f$ and the mass resolution δm can be expressed as [11,12]:

$$\frac{\Delta m}{\Delta f} = -\frac{2m^*}{f}, \tag{2}$$

$$\delta m = \frac{2m^*}{A}\sqrt{\frac{k_B T B}{kQf}}, \tag{3}$$

where m^* is the effective mass of the cantilever ($m^* = nm$, $n = 0.24$ for the fundamental mode of a rectangular cantilever beam, where m is the mass of the cantilever [13]), and A, k_B, T, B, Q denote the amplitude of oscillation, Boltzmann constant, absolute temperature, and the bandwidth, respectively. The higher quality factor the lever has, the smaller mass it can detect.

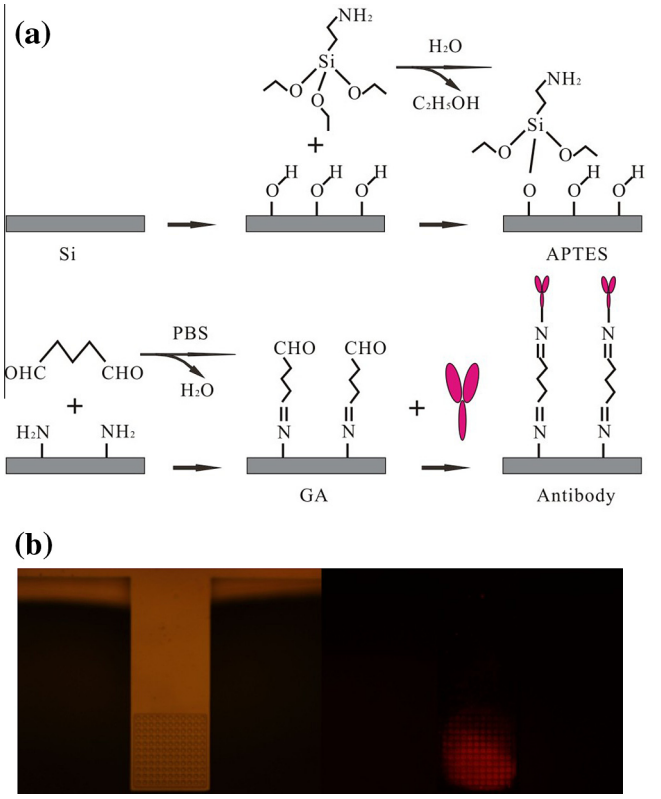

Fig. 4. (a) Functional process of the cantilever surface with AFP antibody, (b) the bright-field and dark-field fluorescent images of the fluorescence CY5 labeled antibody which localized on the micro-cavity.

3.2. Analytical model for multilayer adsorption and surface stress

In the functionalization process, as shown in Fig. 6, a various kind of organic layers, APTES, GA, and BSA, etc, covered the full surface of the cantilever except the locally immobilized antibody, although these organic are small molecular compared to the antibody, they leads to change of the Young's modulus and the cantilever stiffness, finally to the mass detection error. The E_{mc} and k_{mc} of the multilayer cantilever can be expressed as [14]:

$$E_{mc} = \frac{2 \times h_1 \times E_1 + \ldots + 2 \times h_i \times E_i + h_0 \times E_0}{h_0 + 2h_1 + \ldots + 2h_i}, \tag{4}$$

$$k_{mc} = \frac{E_{mc} \times w_{mc} \times h_{mc}^3}{4l_{mc}^3}, \tag{5}$$

where h_i and E_i are the thickness and Young's modulus of the ith organic layer, and w_{mc}, h_{mc}, l_{mc} are the width, thickness, and length of the multilayer cantilever. The thicknesses of APTES, GA, and BSA measured by ellipsometry are 1.04 nm, 0.58 nm, and 2.5 nm, respectively. For the cantilever of $l = 195$ µm, $w = 75$ µm, and $h = 5$ µm, the Young's modulus of the multilayer cantilever is calculated to be 159.7 GPa with $E_0 = 160$ GPa for silicon. The cantilever stiffness changes from 50.57 to 50.49 N/m. This modified k_{mc} value will be applied in the following equation for mass calculation.

Adsorption-induced surface stress is another important factor for the lever stiffness change. Fig. 7 shows schematic for the cantilever covered with a uniform AFP antigen layer, ξ denotes the distance between AFP antibody and antigen molecules, ς is the distance between the adjacent two antibody molecules. There exist intermolecular forces between AFP antigen and the antibody molecules. The van der Waals interaction is one major

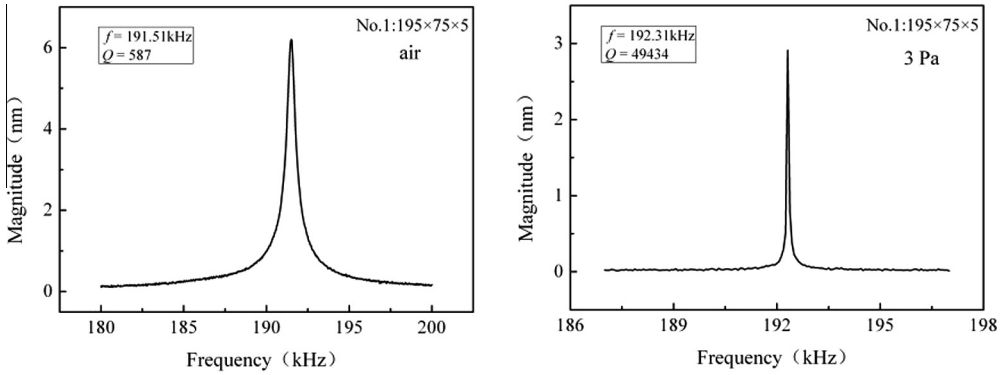

Fig. 5. Resonance spectrum of the cantilever measured in air and in vacuum.

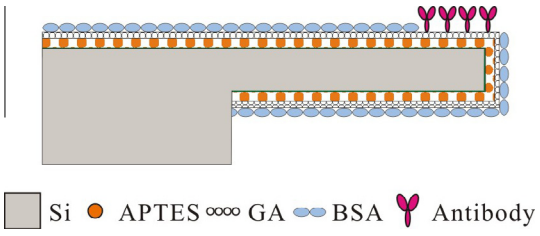

Fig. 6. Schematic of the multilayer cantilever.

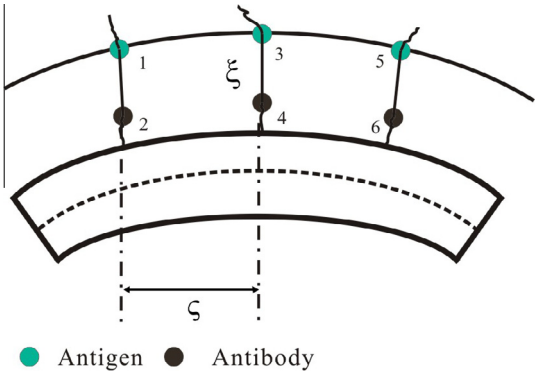

Fig. 7. Schematic for the cantilever covered with a uniform AFP antigen layer.

driving force for adsorption, and can be expressed in term of Lennard-Jones potential [15]:

$$U_L(r_{ij}) = -\frac{A}{r_{ij}^6} + \frac{B}{r_{ij}^{12}}, \tag{6}$$

where r_{ij} is the distance between molecules i and j, A and B are Lennard-Jones constants. On adsorption, the total potential energy of the adsorbate-cantilever system can be expressed as $U = U_L + U_e$, where U_L is the Lennard-Jones potential and U_e is the elastic energy of the bending cantilever caused by small deflection. In the equilibrium state, there is $\partial U/\partial K = 0$ (K denotes the curvature of the cantilever), and the adsorption induced surface stress s can be obtained [16]:

$$s = \frac{\eta}{\varsigma^7}\frac{A}{r_e^4} - \frac{2\eta}{\varsigma^{13}}\frac{B}{r_e^7}, \tag{7}$$

where $r_e = \frac{1}{4} + (\xi/\varsigma)^2$ and η is the distribution density of the AFP antigen on the cantilever surface.

The surface stress on the cantilever leads to the lever stiffness change and is expressed as [17]:

$$\Delta k = \frac{\pi^2}{4}s, \tag{8}$$

thus, the resonance frequency shift resulting from adsorption-induced surface stress and mass change can be computed by:

$$\frac{\Delta f}{f} = \frac{1}{2}\left(\frac{\Delta k}{k_{mc}} - \frac{\Delta m}{m^*}\right), \tag{9}$$

It can be seen from Eq. (9) that the intermolecular van der Waals interaction forces between antigen and antibody change the resonance frequency of the cantilever. In addition, between the AFP antibody and antigen molecules, there exist hydrogen donor, hydrogen acceptor, and hydrophobic groups such as hydroxyl, amidoge, and benzene ring, etc, thus the hydrogen bond and hydrophobic interaction are also the two main intermolecular forces except van der Waals interaction. But it is difficult to quantitatively compute these two forces as the van der Waals interaction due to the tight packing in the interior of folded proteins. Using the above-mentioned analytical model, the van der Waals force can be computed. The hydrogen bond interaction is stronger than the van der Waals interaction, their bond energy are about 20.9 and 7 kJ/mol, respectively [18], so the hydrogen bond interaction is about three times as much as van der Waals interaction. The hydrophobic interaction is about 50% of the overall interaction force [1]. Thus a total intermolecular forces, which is estimated to be about eight times as much as van der Waals force, is applied in the analytical model. The mass of AFP antigen molecule is about 65 kDa, for AFP antigen solution of 18 pg/ml, the intermolecular forces could result in a frequency change of about 40 Hz, the same order of magnitude as that resulting from mass loading of AFP antigen.

3.3. AFP detection

For verifying the performance of the fabricated cantilever-based mass sensor, an 5.5 pg/ml AFP antigen solution is prepared and detected with two different sensor, the first sensor, named as fully immobilized lever, has the antibody immobilized on full cantilever surface, the second sensor, named as locally immobilized lever, has the antibody locally printed in the micro-cavity. Fig. 8 depicts the measured frequency response of fully immobilized lever to the AFP solution, the frequency shift is 830 Hz, about two orders of magnitude larger than the theoretical one 6 Hz, this deviation could mainly be attributed to the lever k variation caused by the AFP adsorption on the whole cantilever.

The frequency response of the locally antibody-immobilized cantilever to AFP antigen solution is given in Fig. 9. The effect of the k variation on the frequency shift is greatly decreased by locally immobilizing the AFP antibody. Using the above-mentioned

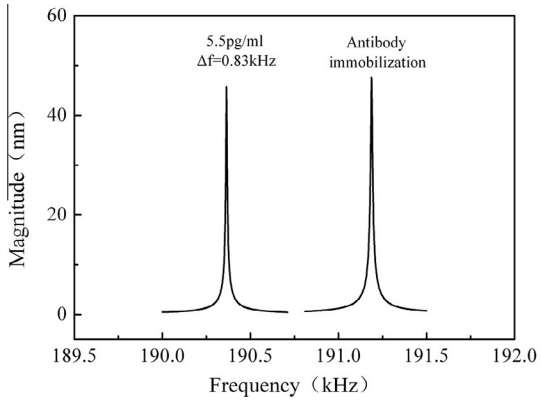

Fig. 8. Frequency response of the fully immobilized lever to the AFP solution of 5.5 pg/ml.

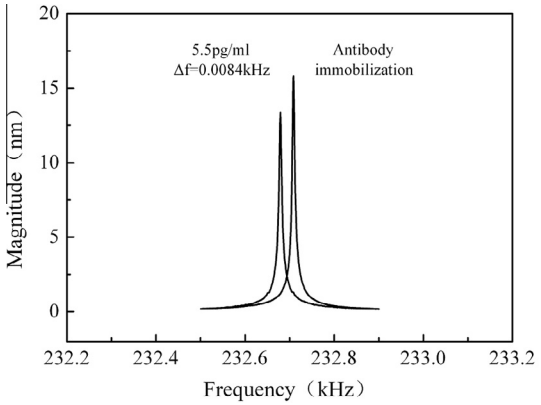

Fig. 9. Frequency shift of the locally antibody-immobilized cantilever responding to the AFP solution of 5.5 pg/ml.

analytical model to further reduce the deviation from k change caused by the multilayer organic and adsorption-induced surface stress, the experimental frequency shift was modified to 8.4 Hz, corresponding to AFP antigen mass of 7.6 pg/ml, quite close to 5.5 pg/ml.

The same method has been applied to detect the AFP antigen solution with various concentrations of 15 and 18 pg/ml, the corresponding AFP antigen mass are 4.4 pg and 5.2 pg, respectively, as shown in Fig. 10, the detected mass with the sensor are 4.5 and 5.35 pg, respectively, quite close to the theoretical values.

Above all, the adsorption induced resonance frequency shift of the cantilever-based sensor working in a dynamic mode depends not only on mass loading but also on variation of the lever stiffness. Therefore, it is important to eliminate the interference of the stiffness change for precise mass detection. The newly developed cantilever-based sensor with the micro-cavity for local reaction and the analytical model for the inter-molecule interaction and multilayer cantilever have effectively eliminated the influence of k variation and significantly improved the detection accuracy and performance of the cantilever-based biosensor. This approach can promote practical application of the cantilever-based sensors. The PCB circuit for processing the output signal of the Wheatstone bridge will be integrated with the cantilever chip to build up a portable cancer diagnosis system in near future.

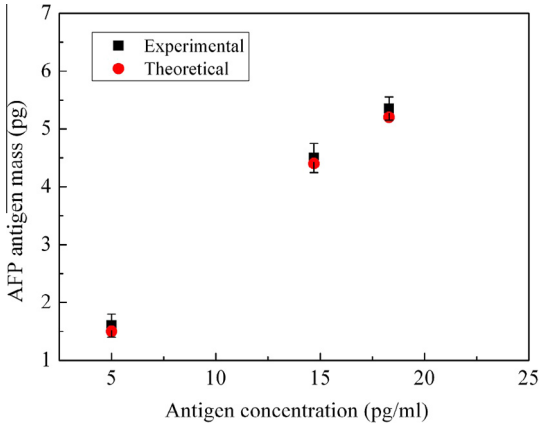

Fig. 10. Sensor response to the AFP antigen solution of 5.5 pg/ml, 15 pg/ml and 18 pg/ml.

4. Conclusion

This work developed a novel cantilever-based biosensor with high sensitivity and mass detection accuracy for early diagnosis of liver cancer. The unique structural features of the biosensor include: cantilever arrays for jointly detecting multi-biomarkers, a micro-cavity in the cantilever for local interaction between antibody and antigen, the pillar arrays for increasing detection upper limit. These structural features offer several advantages: high sensitivity, high throughput, high mass detection accuracy, small volume, and low cost.

The cantilever arrays are batch fabricated with MEMS technology. An analytical model has been established to eliminate the interference of the adsorption-induced stiffness change and has been applied to precise mass detection of cancer biomarker AFP, the experimentally detected AFP antigen mass by the sensor (7.6 pg/ml) is two orders of magnitude smaller than those of the fully antibody-immobilized cantilever sensor, quite close to the calculated one (5.5 pg/ml), These results are significant for pushing forward practical application of the cantilever-based sensors.

Conflict of interest

We declare that we have no conflict of interest.

Acknowledgements

This work is supported by the projects from the Major State Basic Research Development Program of China (973 project: 2011CB933102 and 2013YQ16055103) and the National Science Foundation of China (61234007 and 61201104).

References

[1] J. Arlett, E. Myers, M. Roukes, Comparative advantages of mechanical biosensors, Nat. Nanotech. 6 (4) (2011) 203–215.
[2] R. Raiteri, M. Grattarola, H.-J. Butt, P. Skládal, Micromechanical cantilever-based biosensors, Sens. Actuators, B 79 (2) (2001) 115–126.
[3] M. Alvarez, L.M. Lechuga, Microcantilever-based platforms as biosensing tools, Analyst 135 (5) (2010) 827–836.
[4] A. Hierlemann, O. Brand, C. Hagleitner, H. Baltes, Microfabrication techniques for chemical/biosensors, Proc. IEEE 91 (6) (2003) 839–863.
[5] N.V. Lavrik, M.J. Sepaniak, P.G. Datskos, Cantilever transducers as a platform for chemical and biological sensors, Rev. Sci. Instrum. 75 (7) (2004) 2229–2253.
[6] B.N. Johnson, R. Mutharasan, Biosensing using dynamic-mode cantilever sensors: a review, Biosens. Bioelectron. 32 (1) (2012) 1–18.
[7] J.H. Lee, T.S. Kim, K.H. Yoon, Effect of mass and stress on resonant frequency shift of functionalized Pb (Zr0. 52Ti0. 48) O3 thin film microcantilever for the detection of C-reactive protein, Appl. Phys. Lett. 84 (16) (2004) 3187–3189.
[8] A.K. Gupta, P.R. Nair, D. Akin, M.R. Ladisch, S. Broyles, M.A. Alam, R. Bashir, Anomalous resonance in a nanomechanical biosensor, PNAS 103 (36) (2006) 13362–13367.
[9] K.S. Hwang, K. Eom, J.H. Lee, D.W. Chun, B.H. Cha, D.S. Yoon, T.S. Kim, J.H. Park, Dominant surface stress driven by biomolecular interactions in the dynamical response of nanomechanical microcantilevers, Appl. Phys. Lett. 89 (17) (2006) 173905.
[10] D.F. Wang, T. Ono, M. Esashi, Thermal treatments and gas adsorption influences on nanomechanics of ultra-thin silicon resonators for ultimate sensing, Nanotechnology 15 (12) (2004) 1851.

[11] K.S. Hwang, S.-M. Lee, S.K. Kim, J.H. Lee, T.S. Kim, Micro-and nanocantilever devices and systems for biomolecule detection, Annu. Rev. Anal. Chem. 2 (2009) 77–98.
[12] T. Albrecht, P. Grütter, D. Horne, D. Rugar, Frequency modulation detection using high-Q cantilevers for enhanced force microscope sensitivity, J. Appl. Phys. 69 (2) (1991) 668–673.
[13] T. Thundat, R. Warmack, G. Chen, D. Allison, Thermal and ambient-induced deflections of scanning force microscope cantilevers, Appl. Phys. Lett. 64 (21) (1994) 2894–2896.
[14] N. Snis, E. Edqvist, U. Simu, S. Johansson, Monolithic fabrication of multilayer P (VDF-TrFE) cantilevers, Sens. Actuators, A 144 (2) (2008) 314–320.
[15] P. Sony, P. Puschnig, D. Nabok, C. Ambrosch-Draxl, Importance of van der Waals interaction for organic molecule-metal junctions: adsorption of thiophene on Cu (110) as a prototype, Phys. Rev. Lett. 99 (17) (2007) 176401.
[16] X. Yi, H. Duan, Surface stress induced by interactions of adsorbates and its effect on deformation and frequency of microcantilever sensors, JMPS 57 (8) (2009) 1254–1266.
[17] G. Chen, T. Thundat, E. Wachter, R. Warmack, Adsorption-induced surface stress and its effects on resonance frequency of microcantilevers, J. Appl. Phys. 77 (8) (1995) 3618–3622.
[18] P.E. Wormer, A. van der Avoird, Intermolecular potentials, internal motions, and spectra of van der Waals and hydrogen-bonded complexes, Chem. Rev. 100 (11) (2000) 4109–4144.